Fossil Record 12 (2) 2009, 197–205 / DOI 10.1002/mmng.200900007

WILEY-VCH

museum für naturkunde

Stratigraphic significance of carbon isotope variations in the shallow-marine Seis/Siusi Permian–Triassic boundary section (Southern Alps, Italy)

Sonja H. Kraus*,[1], Susann Siegert[1], Wolfgang Mette[2], Ulrich Struck[3] and Christoph Korte[1]

[1] Institut für Geologische Wissenschaften, Freie Universität Berlin, Malteserstr. 74–100, 12249 Berlin, Germany.
E-mail: sonja.kraus@t-online.de
[2] Institut für Geologie und Paläontologie, Universität Innsbruck, Innrain 52, 6020 Innsbruck, Austria
[3] Museum für Naturkunde Berlin, Invalidenstraße 43, 10115 Berlin, Germany

Abstract

Carbonate carbon-isotope values from the Permian–Triassic (P–T) boundary section at Seis/Siusi (Southern Alps, Italy) show a trend similar to that in numerous other P–T boundary sections worldwide. Values decrease from 3.2 ‰ (V-PDB) in the upper *Bellerophon* Limestone Formation (Late Permian) to a minimum of −1.7 ‰ in the lower Mazzin Member. This minimum may represent the P–T boundary. The overall declining carbon-isotope trend is interrupted by a ca. 1 ‰ positive excursion in the higher Tesero Oolite Horizon. This positive peak is located at a higher lithostratigraphic level than a comparable peak in the adjacent Pufels section, which suggests that the Tesero Oolite Horizon in the Seis section is stratigraphically slightly older than in the Pufels section, and this is also suggested by palaeomagnetic correlation. It is therefore concluded that the base of the Tesero Oolite Horizon does not reflect a synchronous "current event" but is slightly diachronous, a result that was previously shown by biostratigraphic correlation. Nevertheless, this suggestion should be verified by further detailed litho-, magneto- and chemostratigraphic analysis of other P–T sections in the Southern Alps.

Received 12 March 2009
Accepted 24 March 2009
Published 3 August 2009

Key Words

chemostratigraphy
extinction events
oolites
Pufels section
Seis section

Introduction

The most severe mass extinction of the Phanerozoic affected marine and continental biota in the latest Permian, close to the Permian–Triassic (P–T) boundary (e.g., Schindewolf 1953; Sepkoski 1989; Raup 1991; Erwin 2006; Kozur 1998a). This event was accompanied by spectacular global environmental changes, involving significant perturbations of Earth's carbon cycle expressed as a prominent negative carbon-isotope excursion (e.g., Chen et al. 1984; Holser & Magaritz 1987; Magaritz et al. 1988; Holser et al. 1989; Oberhänsli et al. 1989; Wang et al. 1994; Morante 1996; Wignall et al. 1998; Heydari et al. 2000; Krull & Retallack 2000; Krull et al. 2000; Twitchett et al. 2001; Musashi et al. 2001; Wit et al. 2002; Sephton et al. 2002; Korte et al. 2004a, 2004b, 2004c, 2005, 2009; Thomas et al. 2004; Korte & Kozur 2005a, 2005b; Algeo et al. 2007a, 2007b; Coney et al. 2007; Riccardi et al. 2007). Because of its expression in marine and continental carbonates and in organic matter, it is generally accepted that this negative $\delta^{13}C$ excursion is global in scale. However, what actually triggered the P–T boundary $\delta^{13}C$ trend is still under discussion. Several possible causes, such as Siberian Trap volcanism (e.g., Renne et al. 1995; Kozur 1998a, 1998b; Svensen et al. 2004; Hansen 2006; Payne & Kump 2007; Retallack & Jahren 2008; Korte et al. 2009), re-mobilisation of formerly deposited ^{13}C-depleted organic material due to enhanced weathering triggered by sea-level fall (e.g., Holser & Magaritz 1992), dissociation of isotopically light methane clathrates (e.g., Erwin 1994; Krull & Retallack 2000; Krull et al. 2000; Twitchett et al. 2001; Wit et al. 2002; Sarkar et al. 2003), a collapse in primary oceanic productivity (e.g., Visscher et al. 1996; Rampino & Caldeira 2005), and shallow marine anoxia resulting

* Corresponding author

from an upward rise in the chemocline or ocean overturn (Malkowski et al. 1989; Korte et al. 2004a; Kump et al. 2005; Algeo et al. 2007a, 2008) have been suggested. It is most likely that more than one trigger was responsible for the −4 to −7 ‰ negative excursion (e.g., Renne et al. 1995; Berner 2002; Korte et al. 2004a; Sephton et al. 2005). Factors that might at this time have affected the global carbon cycle and other aspects of the Earth system, are discussed extensively (e.g., Erwin et al. 2002; Benton 2003; Benton & Twitchett 2003; Kump 2003; Corsetti et al. 2005; Racki & Wignall 2005; Erwin 2006; Isozaki 2007; Twitchett 2007; Wignall 2007; Korte & Kozur 2009).

Carbon-isotope excursions, if global in scale, are detectable in marine and continental sediments and, because of the short residence times of carbon in ocean and atmosphere, can be used for stratigraphic correlation. Here, we present carbon-isotope values for the shallow-marine Permian–Triassic boundary section at Seis/Siusi (Southern Alps, Italy). We have used the carbon-isotope trend to correlate the Seis section with other P–T boundary successions of the Southern Alps and elsewhere. As a result, we propose new stratigraphic findings for the Seis section that bear on latest Permian deposition in the Dolomites.

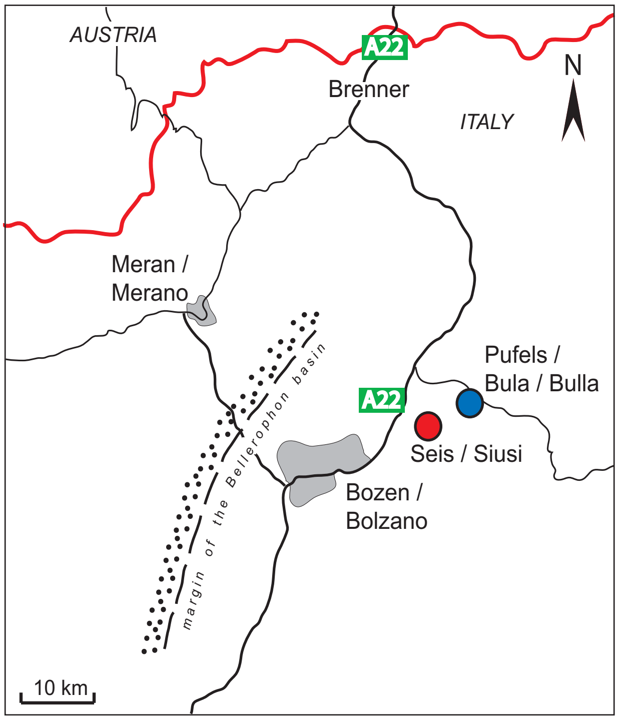

Figure 1. Map of the studied locality at Seis/Siusi and adjacent coeval section at Pufels/Bula/Bulla, both Southern Alps, Italy. Map modified after Brandner (1988).

Geological settings and stratigraphic background

Bulk carbonate samples were collected in September 2007 and June 2008 in a section about 1 km south of Seis (Siusi) village, Dolomites, Southern Alps, Italy (Fig. 1). At the end of the Permian this location was situated on an inner carbonate ramp (Noé 1987; Brandner 1988; Newton et al. 2004) at the westernmost margin of the Palaeotethys, near the equator (Fig. 2). The succession consists of dolomitic mudstones and wackestones of the upper *Bellerophon* Limestone Formation (Fig. 3), followed upwards by grainstones, mudstones and marls of the Werfen Formation, including the Tesero Oolite Horizon (TOH), and subsequently by mudstones of the lower Mazzin Member. The shallow water deposits are characterised by continuous and relatively high sedimentation rates compared to the classical P–T boundary sections such as S-China, Iran and Perigondwanan localities (Atudorei 1999; Yin et al. 2001; Kozur 2007). These conditions represent an excellent environment for carbonate sedimentation (Noé 1987) and make high-resolution carbon-isotope sampling possible.

The base of the Triassic is defined by the International Commission on Stratigraphy by the first appearance datum (FAD) of the conodont *Hindeodus parvus* (Kozur & Pjatakova, 1976). Conodonts are rare in the Late Permian and Early Triassic succession of the Southern Alps; thus, it is difficult to define biozones precisely. However, the occurrence of *Hindeodus* and *Isarcicella* allows a subdivision of the stratigraphic record into the *H. praeparvus* Zone, the *H. parvus* Zone and the *I. isarcica* Zone at the Pufels, Tesero and at the Gartnerkofel core locations (Perri 1991; Schönlaub 1991; Farabegoli & Perri 1998; Nicora & Perri 1999; Korte & Kozur 2005a; Korte et al. 2009).

Formerly, the P–T boundary was lithostratigraphically placed between the *Bellerophon* Limestone and the Werfen Beds at the base of the TOH (e.g., Leonardi

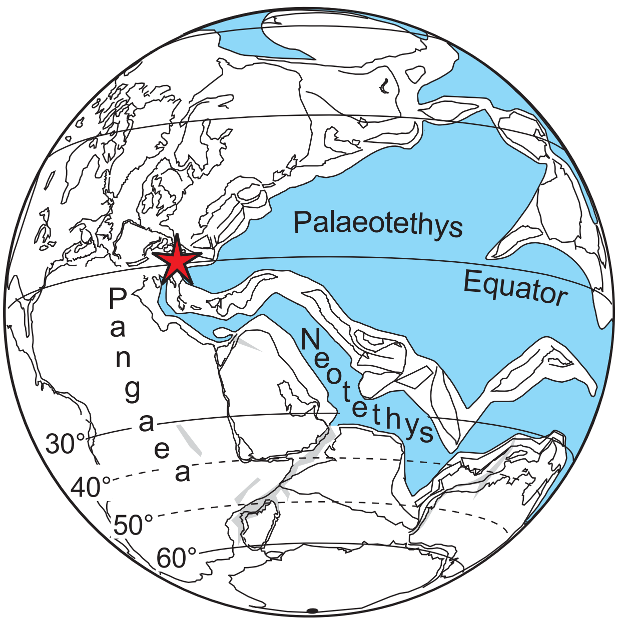

Figure 2. Palaeogeographic map of the Late Permian at 260 Ma [modified after Stampfli and Borel (2002) and Korte et al. (2008)] with sampled region (Southern Alps, Italy: star).

1967; Bosellini & Hardie 1973), but the FAD of *H. parvus*, and with it the P–T boundary, is distinctly higher and lies within the Mazzin Member (Kozur 1989, 1995, 1996, 1998a, 1998b; Perri 1991; Farabegoli & Perri 1998; Korte & Kozur 2005a; Korte et al. 2009).

Methods

Powders were drilled from fresh surfaces of bulk carbonates. Samples of approximately 100–400 µg were filled into clean 10 ml exetainers and sealed with a septum cap (caps and septa for LABCO exetainer 438b). The remaining air was removed by flushing the exetainer with

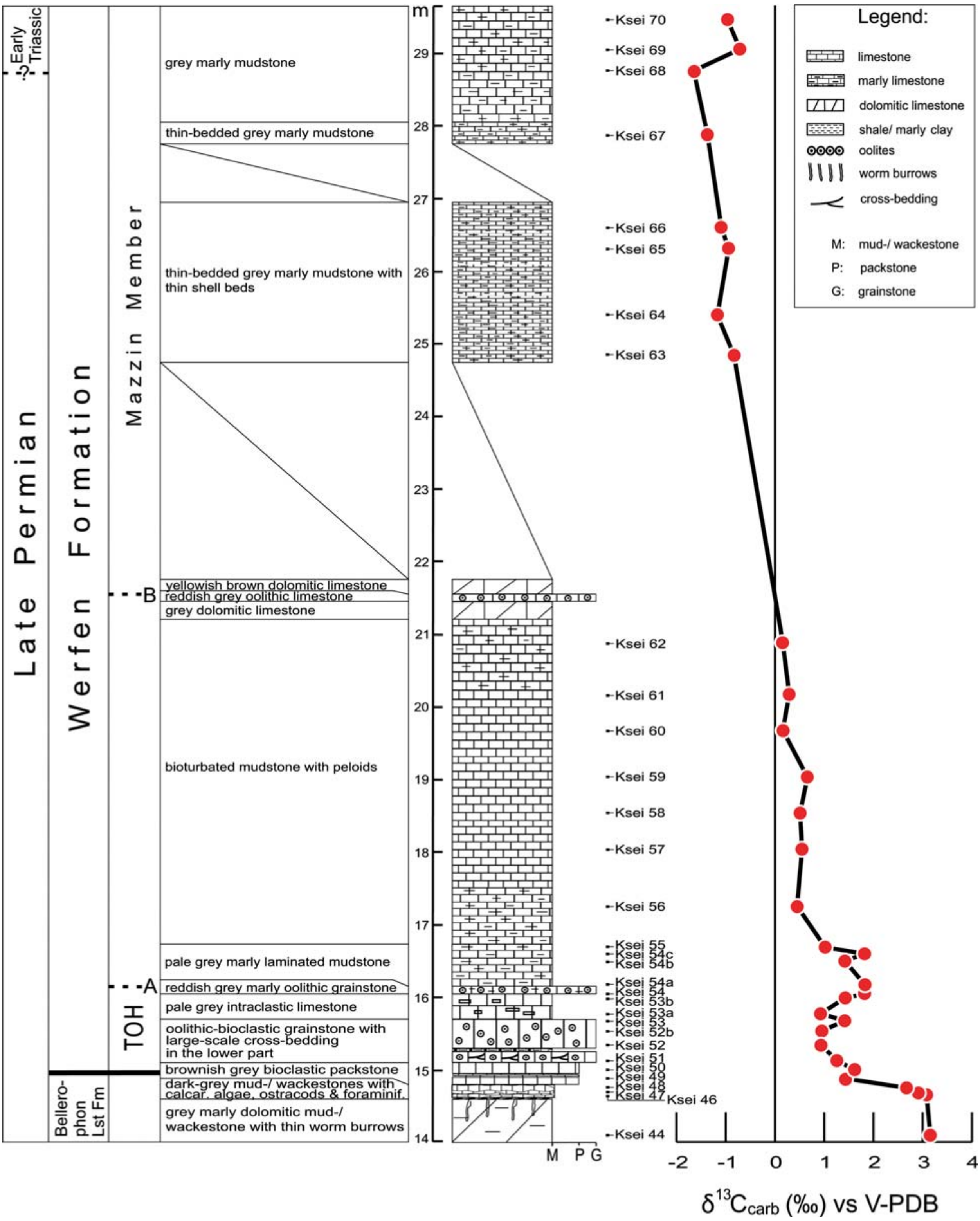

Figure 3. Seis/Siusi section, showing lithology, sample locations, and carbon isotope values for bulk carbonates.

Table 1. Carbon and oxygen isotope values of investigated samples.

Sample no.	$\delta^{13}C_{carb}$ vs V-PDB [‰]	$\delta^{18}O$ vs V-SMOW [‰]
Ksei 44	3.16	27.26
Ksei 46	3.08	24.75
Ksei 47	2.92	25.55
Ksei 48	2.67	25.40
Ksei 49	1.44	23.73
Ksei 50	1.62	24.25
Ksei 51	1.26	23.46
Ksei 52	0.94	24.61
Ksei 52b	0.95	24.72
Ksei 53	1.42	26.21
Ksei 53a	0.93	24.94
Ksei 53b	1.43	25.74
Ksei 54	1.82	25.13
Ksei 54a	1.83	26.01
Ksei 54b	1.42	26.57
Ksei 54c	1.82	28.09
Ksei 55	1.02	25.24
Ksei 56	0.45	26.44
Ksei 57	0.55	25.87
Ksei 58	0.51	25.17
Ksei 59	0.66	25.90
Ksei 60	0.16	27.42
Ksei 61	0.29	25.35
Ksei 62	0.16	25.22
Ksei 63	−0.83	26.78
Ksei 64	−1.17	25.63
Ksei 65	−0.94	24.96
Ksei 66	−1.09	24.58
Ksei 67	−1.37	25.86
Ksei 68	−1.65	25.15
Ksei 69	−0.71	28.52
Ksei 70	−0.96	26.55

He (4.6) for 6 min at a flow of 100 µl per minute. Subsequently, about 30 l of anhydrous phosphoric acid was injected through the septum into the sealed exetainer by using a disposable syringe. The CO_2 of the reacted carbonate was analysed for $\delta^{18}O$ and $\delta^{13}C$ on a Thermo Finnigan GASBENCH II coupled online with a Thermo Finnigan DELTA V isotope ratio mass spectrometer. Reference gas was measured using a pure CO_2 (4.5) from a cylinder and calibrated against the V-PDB standard by using IAEA reference materials (NBS 18, NBS 19). The reproducibility of replicated standards is typically better than 0.1 ‰ (one standard deviation) for $\delta^{13}C$ and $\delta^{18}O$. Carbon- and oxygen-isotope values were calibrated against V-PDB and are reported in the standard ‰-notation (Tab. 1).

Results

Carbon isotope values from homogeneous micritic carbonates in the Seis section between the latest *Bellerophon* Limestone Formation and the lower Mazzin Member (Fig. 3; Tab. 1) vary between 3.2 and −1.7 ‰ (V-PDB). A general trend towards lower $\delta^{13}C$ values is discernible upward throughout the investigated section. This trend is interrupted by a short-term, positive excursion starting with an amplitude of about 1 ‰ (from 0.9 to 1.8 ‰) about 1 m above the base of the TOH. This positive excursion occurs over a stratigraphic thickness of about 1 m; the subsequent decline in $\delta^{13}C$ values reaches a minimum of −1.7 ‰ about 14 m above the base of the TOH (sample Ksei 68). The two samples above this minimum show a slight trend towards higher $\delta^{13}C$ values.

Discussion

The carbon-isotope data from the Seis/Siusi section show the same feature that was recently proposed as the “general P–T boundary trend” obtained from numerous P–T boundary sections worldwide (Korte et al. 2009). The decrease of $\delta^{13}C$ values in this general trend is evident already in the Late Permian (late Changhsingian) *C. bachmanni* Zone, lasted several 100,000 years, and reaches a first minimum at the P–T boundary. Therefore, in the absence of conodonts, the lowest value in the $\delta^{13}C$ curve can be utilized to define the P–T boundary (Korte & Kozur 2009; Korte et al. 2009). Thus it is possible that the minimum of −1.7 ‰ at sample Ksei 68 (~14 m above the base of the TOH) represents the P–T boundary. At the Pufels section, a similar $\delta^{13}C$ minimum (−2.7 ‰) occurs at about 12 m above the base of the TOH (Horacek et al. 2007); this has been proposed to represent the P–T boundary minimum (Korte et al. 2009) using conodont stratigraphic ranges from Mostler (1982), Perri (1991), Farabegoli & Perri (1998), Farabegoli et al. (2007) and Kozur in Korte et al. (2009). Two factors, however, render the chemostratigraphic definition of the P–T boundary at Seis uncertain: (1) the $\delta^{13}C$ minimum value at Pufels is more than 1 ‰ lower, and (2) the position of the minimum with respect to the base of the TOH is somewhat lower at Pufels, although a slightly higher sedimentation rate for Pufels (in comparison to Seis) can be inferred for the latest *Bellerophon* Limestone Formation (Brandner pers. comm. 2009). It is therefore possible that the P–T boundary at Seis lies slightly lower (or higher) than the $\delta^{13}C$ minimum (no data available). On the other hand, it is still a matter for discussion whether the TOH is actually diachronous.

Assereto et al. (1973) assumed that the lithologic change from the *Bellerophon* Limestone Formation to the TOH (the previous P–T boundary in the Southern Alps) is diachronous (see also Wignall & Hallam 1992; Kozur 1994; Korte & Kozur 2005a). In contrast, Scholger et al. (2000) proposed that the boundary between the *Bellerophon* Limestone Formation and the TOH is an isochronous boundary *sensu stricto*. The new carbon-isotope values contribute to this discussion. In several P–T boundary sections, such as Meishan B (Nan & Liu 2004), Abadeh (Korte et al. 2004a), Shahreza (Korte et al. 2004b), Zal (Korte et al. 2004c), Gartnerkofel core (Holser et al. 1989) or Guryul Ravine (Korte et al. 2009), the latest Permian decreasing $\delta^{13}C$ trend is interrupted by a positive excursion of about 1 ‰ magnitude starting somewhat below or at the main extinction event (= event horizon). This short-term positive trend is also recognisable in the $\delta^{13}C$ values from Seis between samples 53a and 56 (Fig. 3). Because of this similarity we believe that this 1 ‰ positive carbon isotope excursion may be global in extent. This chemostratigraphic marker may therefore be excellently suited for stratigraphic correlation within the interval of interest. A comparison of the carbon isotope curves of the Seis section (this study) and at Pufels (Korte & Kozur 2005a), as well as the lithology and magnetic polarity (the later published by Scholger et al. 2000), indicates that the short-term positive excursion at Seis (Fig. 4) starts about 0.8 m above the base of the TOH (Fig. 4) at sample 53a (Fig. 3). In contrast, the same positive excursion starts at Pufels (not expressed by Gorjan et al. 2008) right after the first oolite bed about 0.2 m above the base of the TOH. These results indicate that the TOH at Seis was deposited slightly earlier than at Pufels. This finding is the more remarkable because the compared sections are less than 10 km apart from each other (Fig. 1). The result would also imply that the TOH is a regressive unit since the litho- and biofacies at the Seis section reflect a shallower water depth than the more easterly Pufels section. During this regression, the distal localities in the east were characterized by later occurrence of shallow-water oolite facies than the sections in the west, which were situated closer to the palaeocoast (Fig. 1). These suggestions confirm biostratigraphic results by Kozur (1994). However, further chemo- and magnetostratigraphic studies of southern alpine P–T boundary sections are desirable to verify these results.

It has been proposed that the oolites were not the result of a transgression or regression, but accumulated due to sudden climate and/or oceanography changes ("current event", see Brandner 1988; Brandner et al. 2008). The marly layer about 0.3 m above the base of the TOH at Seis (Figs 4 and 5) may represent the marly layer at about 0.2 m above the base of the TOH at Pufels (Fig. 4) (Brandner pers. comm. 2009). If this is the case, the temporal difference in the deposition of the oolites between Seis and Pufels may not be resolvable because of the deposition of these beds must be contemporaneous. This explanation, however, cannot be confirmed by the carbon-isotope data because the short-term positive excursion is distinctly higher in Seis than in Pufels.

The main extinction event in the latest Permian, recognisable in several P–T boundary sections (e.g., Meishan, China: Yin et al. 2001; Abadeh, Jolfa, Shahreza, Zal, all Iran: Kozur 2007), occurs abruptly at the base of the *C. meishanensis* – *H. praeparvus* Zone, a stratigraphic level coeval with the base of the Boundary Clay. It is difficult to define this (equivalent) biostratigraphic base at the Seis section and, in addition, the Boundary Clay is not developed because of the shallow water. At the Pufels section, the biotas were seriously affected near the base of the TOH (Farabegoli et al. 2007) and the same can be observed at the Seis section. It is, however, most likely that the biota at Pufels and Seis disappeared because of the onset of high energy conditions in shallow water with formation of compact oolites at both locations. Similar facies changes also cause strong local biotic change within the Permian and Triassic. The real main extinction event was certainly not situated at the base of the TOH, but within the Werfen Beds. This can be stated because fusulinids and Permian holothurian sclerites do not occur elsewhere

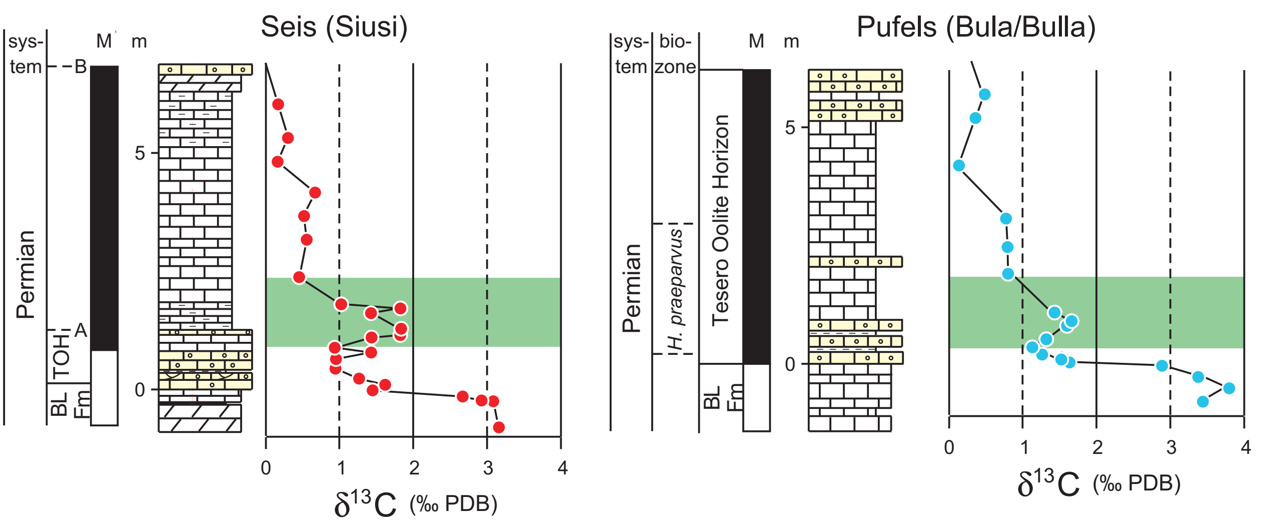

Figure 4. Lithology, carbon isotope values, and magnetic polarity (M; white: reversed interval; black: normal interval) of the Seis/Siusi and Pufels/Bula/Bulla sections in the latest *Bellerophon* Limestone Formation (BL Fm) and the Tesero Oolite Horizon (TOH). The carbon isotope data for Pufels originate from Korte & Kozur (2005a) and the magnetostratigraphic results (M) for both sections are from Scholger et al. (2000). Boundary between TOH and Mazzin Member: (A): Scholger et al. (2000); (B): Newton et al. (2004). This figure is available in colour online at: museum-fossilrecord.wiley-vch.de.

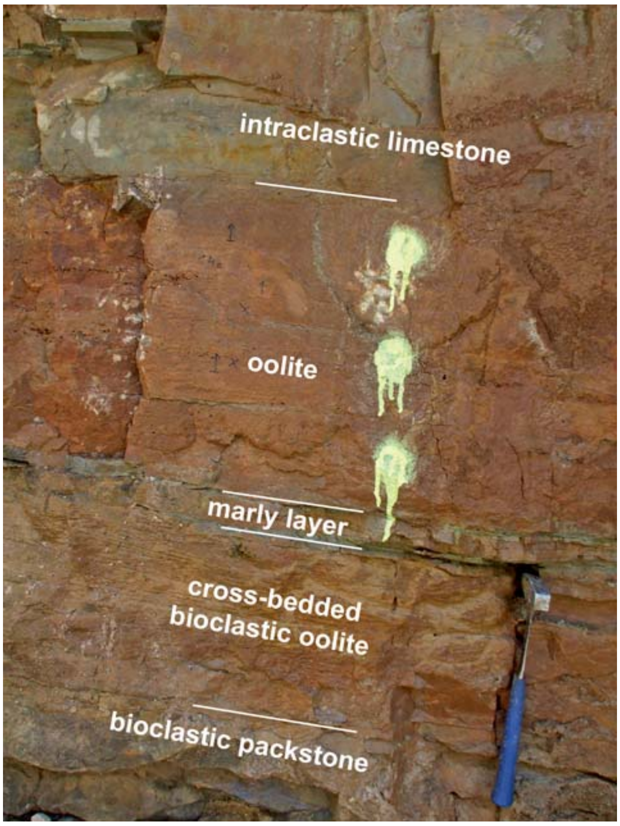

Figure 5. Photograph of the TOH at Seis with subdivision in logged beds. This figure is available in colour online at: museum-fossilrecord.wiley-vch.de.

above the main extinction event, but are present within the TOH (Kozur 1994). The disappearance of biota near the base of the TOH at Seis and Pufels therefore does not chronostratigraphically correspond to the event horizon of the Chinese or Iran sections.

Palaeomagnetic data (Scholger et al. 2000) can also be used for correlation. These show that a short palaeomagnetic reversed interval is followed by a long normal interval that straddles the P–T boundary (Fig. 4). This polarity-change is biostratigraphically defined in other sections and occurs in the Germanic Basin (Szurlies 2004; Bachmann & Kozur 2004) somewhat below the main extinction event in the Tethys. The palaeomagnetic data of Scholger et al. (2000) for Seis and Pufels also suggest a diachronous boundary between the *Bellerophon* Limestone Formation and the TOH (Fig. 4). At the Seis section, the change from reversed to normal polarity occurs either within the upper TOH, distinctly above the top of the *Bellerophon* Limestone Formation or, maybe, even within the lower Mazzin Member (but note that Newton et al. (2004) drew the boundary between TOH and the Mazzin Member distinctly higher than Scholger et al. (2000); see Fig. 4). At the Pufels section, this change in polarity occurs close to the base of the TOH (first normal magnetised sample 5 cm above the base of the TOH). These results confirm the interpretation of the carbon-isotope values and suggest that the boundary between the *Bellerophon* Limestone Formation and the TOH is diachronous and the lower part of the TOH at Seis corresponds to the latest *Bellerophon* Limestone Formation at Pufels.

Conclusion

The latest Permian short-term positive carbon-isotope excursion at the Seis section is situated lithostratigraphically higher than at the adjacent Pufels section. This suggests that the Tesero Oolite Horizon in the Seis section is older than in Pufels, suggesting in turn that the *Bellerophon* Limestone Formation – TOH boundary is diachronous.

Acknowledgements

We acknowledge E. Kuhl (Berlin) for technical assistance, R. Brandner (Innsbruck), C. Heubeck (Berlin), S. P. Hesselbo (Oxford) and H. Mostler (Innsbruck) for discussion, and H. W. Kozur (Budapest) and P. Wignall (Leeds) for the reviews and pertinent comments. We thank the Freie Universität Berlin for contributions to financing this project and for providing the necessary facilities.

References

Algeo, T. J., Ellwood, B., Nguyen, T. K. T., Rowe, H. & Maynard, J. B. 2007a. The Permian–Triassic boundary at Nhi Tao, Vietnam: Evidence for recurrent influx of sulfidic watermasses to a shallow-marine carbonate platform. – Palaeogeography, Palaeoclimatology, Palaeoecology 252: 304–327.

Algeo, T. J., Hannigan, R., Rowe, H., Brookfield, M., Baud, A., Krystyn, L. & Ellwood, B. B. 2007b. Sequencing events across the Permian–Triassic boundary, Guryul Ravine (Kashmir, India). – Palaeogeography, Palaeoclimatology, Palaeoecology 252: 328–346.

Algeo, T., Shen Yanan, Zhang Tonggang, Lyons, T., Bates, S., Rowe, H. & Nguyen, T. K. T. 2008. Association of ^{34}S-depleted pyrite layers with negative carbonate δ^{13}C excursions at the Permian–Triassic boundary: Evidence for upwelling of sulfidic deep-ocean water masses. – Geochemistry Geophysics Geosystems 9: Q04025, doi:10.1029/2007GC001823.

Assereto, R., Bosellini, A., Fantini Sestini, N. & Sweet, W. C. 1973. The Permian–Triassic boundary in the Southern Alps (Italy). *In* Logan, A. & Hills, V. (eds). The Permian and Triassic Systems and their Mutual Boundary. – Canadian Society of Petroleum Geologists Memoir 2: 176–199.

Atudorei, N.-V. 1999. Constraints on the Upper Permian to Upper Triassic marine carbon isotope curve. Case studies from the Tethys. PhD Thesis, University of Lausanne.

Bachmann, G. H. & Kozur, H. W. 2004. The Germanic Triassic: correlations with the international scale, numerical ages and Milankovitch cyclicity. – Hallesches Jahrbuch für Geowissenschaften B 26: 17–62.

Benton, M. J. 2003. When life nearly died. The greatest mass extinction of all time. Thames & Hudson, London.

Benton, M. J. & Twitchett, R. J. 2003. How to kill (almost) all life: the end-Permian extinction event. – Trends in Ecology and Evolution 18: 358–365.

Berner, R. A. 2002. Examination of hypotheses for the Permo–Triassic boundary extinction by carbon cycle modeling. – Proceedings of National Academic Science of the United States of America 99: 4172–4177.

Bosellini, A. & Hardie, A. L. 1973. Depositional theme of a marginal marine evaporite. – Sedimentology 20: 5–27.

Brandner, R. 1988. The Permian–Triassic boundary in the Dolomites (Southern Alps, Italy), San Antonio section. *In* IGCP-Project 199: Rare events in geology. – Berichte der Geologischen Bundesanstalt 15: 49–56.

Brandner, R., Horacek, M., Scholger, R. & Keim, L. 2008. The Pufels/Bulla section: a standard for Permian–Triassic boundary and Lower Triassic in Werfen facies. *In* Kustatscher, E. (ed.). The Triassic Climate, Workshop on Triassic palaeoclimatology, Bozen 3.–7. June 2008. Field Trip Guide, Naturmuseum Südtirol, Bozen 2008.

Chen Jin-shi, Shao Mao-rong, Huo Wei-guo & Yao Yu-yuan. 1984. Carbon isotope of carbonate strata at Permian–Triassic boundary in Changxing, Zhejiang. – Scientia Geologica Sinica 19 (1): 88–93 [in Chinese with English abstract].

Coney, L., Reimold, W. U., Hancox, P. J., Mader, D., Koeberl, C., McDonald, I., Struck, U., Vajda, V. & Kamo, S. L. 2007. Geochemical and mineralogical investigation of the Permian–Triassic boundary in the continental realm of the southern Karoo Basin, South Africa. – Palaeoworld 16: 67–104.

Corsetti, F. A., Baud, A., Marenco, P. J. & Richoz, S. 2005. Summary of Early Triassic carbon isotope records. – Comptes Rendus Palevol 4: 473–486.

Erwin, D. H. 1994. The Permo–Triassic extinction. – Nature 367: 231–236.

Erwin, D. H. 2006. Extinction – How life on earth nearly ended 250 million years ago. Princeton University Press, Princeton and Oxford.

Erwin, D. H., Bowring, S. A. & Jin Yu-gan. 2002. End-Permian mass extinctions: A review. *In* Koeberl, C. & MacLeod, K. G. (eds). Catastrophic events and mass extinctions: Impacts and beyond. – Geological Society of America, Special Paper 356: 363–383.

Farabegoli, E. & Perri, M. C. 1998. Stop 4.3 – Permian/Triassic boundary and Early Triassic of the Bulla section (Southern Alps, Italy): Lithostratigraphy, facies and conodont biostratigraphy. – Giornale di Geologia Ser. 3ª (special issue, ECOS VII Southern Alps Fieldtrip Guidebook) 60: 292–311.

Farabegoli, E., Perri, M. C. & Posenato, R. 2007. Environmental and biotic changes across the Permian–Triassic boundary in western Tethys: The Bulla parastratotype, Italy. – Global and Planetary Change 55: 109–135.

Gorjan, P., Kaiho, K. & Chen, Z.-Q. 2008. A carbon-isotopic study of an end-Permian mass-extinction horizon, Bulla, northern Italy: a negative $\delta^{13}C$ shift prior to the marine extinction. – Terra Nova 20: 253–258.

Hansen, H. J. 2006. Stable isotopes of carbon from basaltic rocks and their possible relation to atmospheric isotope excursions. – Lithos 92: 105–116.

Heydari, E., Hassandzadeh, J. & Wade, W. J. 2000. Geochemistry of central Tethyan Upper Permian and Lower Triassic strata, Abadeh region, Iran. – Sedimentary Geology 137: 85–99.

Holser, W. T. & Magaritz, M. 1987. Events near the Permian–Triassic boundary. – Modern Geology 11: 155–180.

Holser, W. T. & Magaritz, M. 1992. Cretaceous/Tertiary and Permian/Triassic boundary events compared. – Geochimica et Cosmochimica Acta 56: 3297–3309.

Holser, W. T., Schönlaub, H.-P., Attrep, M., Boeckelmann, K., Klein, P., Magaritz, M., Orth, C. J., Fenninger, A., Jenny, C., Kralik, M., Mauritsch, H., Pak, E., Schramm, J.-M., Stattegger, K. & Schmöller, R. 1989. A unique geochemical record at the Permian/Triassic boundary. – Nature 337: 39–44.

Horacek, M., Brandner, R. & Abart, R. 2007. Carbon isotope record of the P/T boundary and the Lower Triassic in the Southern Alps: Evidence for rapid changes in storage of organic carbon. – Palaeogeography, Palaeoclimatology, Palaeoecology 252: 347–354.

Isozaki, Y. 2007. Plume winter scenario for biosphere catastrophe: The Permo–Triassic boundary case. *In* Yuen, D. A., Maruyama, S., Karato, S. & Windley, B. F. (eds). Superplumes: Beyond Plate Tectonics. Springer, Dordrecht: pp. 409–440.

Korte, C. & Kozur, H. W. 2005a. Carbon isotope stratigraphy across the Permian/Triassic boundary at Jolfa (NW-Iran), Peitlerkofel (Sas de Pütia, Sass de Putia), Pufels (Bula, Bulla), Tesero (all three Southern Alps, Italy) and Gerennavár (Bükk Mts., Hungary). – Journal of Alpine Geology 47: 119–135.

Korte, C. & Kozur, H. W. 2005b. Carbon isotope trends in continental lake deposits of uppermost Permian to Lower Olenekian Germanic Lower Buntsandstein (Calvörde and Bernburg Formations). – Hallesches Jahrbuch für Geowissenschaften B, Beiheft 19: 87–94.

Korte, C. & Kozur, H. W. 2009. Carbon isotope stratigraphy across the Permian–Triassic boundary: A review. – Journal of Asian Earth Science (in press).

Korte, C., Kozur, H. W., Joachimski, M. M., Strauss, H., Veizer, J. & Schwark, L. 2004a. Carbon, sulfur, oxygen and strontium isotope records, organic geochemistry and biostratigraphy across the Permian/Triassic boundary in Abadeh, Iran. – International Journal of Earth Sciences 93: 565–581.

Korte, C., Kozur, H. W. & Mohtat-Aghai, P. 2004b. Dzhulfian to lowermost Triassic $\delta^{13}C$ record at the Permian/Triassic boundary section at Shahreza, Central Iran. – Hallesches Jahrbuch für Geowissenschaften B, Beiheft 18: 73–78.

Korte, C., Kozur, H. W. & Partoazar, H. 2004c. Negative carbon isotope excursion at the Permian/Triassic boundary section at Zal, NW-Iran. – Hallesches Jahrbuch für Geowissenschaften B, Beiheft 18: 69–71.

Korte, C., Kozur, H. W. & Veizer, J. 2005. $\delta^{13}C$ and $\delta^{18}O$ values of Triassic brachiopods and carbonate rocks as proxies for coeval seawater and palaeotemperature. – Palaeogeography, Palaeoclimatology, Palaeoecology 226: 287–306.

Korte, C., Jones, P. J., Brand, U., Mertmann, D. & Veizer, J. 2008. Oxygen isotope values from high latitudes: clues for Permian sea-surface temperature gradients and Late Palaeozoic deglaciation. – Palaeogeography, Palaeoclimatology, Palaeoecology 269: 1–16.

Korte, C., Pande, P., Kalia, P., Kozur, H. W., Joachimski, M. M. & Oberhänsli, H. 2009. Massive volcanism at the Permian–Triassic boundary and its impact on the isotopic composition of the ocean and atmosphere. – Journal of Asian Earth Science (in press).

Kozur, H. W. 1989. The Permian–Triassic boundary in marine and continental sediments. – Zentralblatt für Geologie und Paläontologie, Teil 1, 1988 (11/12): 1245–1277.

Kozur, H. W. 1994. The correlation of the Zechstein with the marine standard. – Jahrbuch der Geologischen Bundesanstalt 137: 85–103.

Kozur, H. W. 1995. Some remarks to the conodonts *Hindeodus* and *Isarcicella* in the latest Permian and earliest Triassic. – Palaeoworld 6: 64–77.

Kozur, H. W. 1996. The conodonts *Hindeodus*, *Isarcicella* and *Sweetohindeodus* in the uppermost Permian and lowermost Triassic. – Geologia Croatica 49 (1): 81–115.

Kozur, H. W. 1998a. Some aspects of the Permian–Triassic boundary (PTB) and of the possible causes for the biotic crisis around this boundary. – Palaeogeography, Palaeoclimatology, Palaeoecology 143: 227–272.

Kozur, H. W. 1998b. Problems for evaluation of the scenario of the Permian–Triassic boundary biotic crisis and of its causes. – Geologia Croatica 51/2: 135–162.

Kozur, H. W. 2007. Biostratigraphy and event stratigraphy in Iran around the Permian–Triassic Boundary (PTB): Implications for the causes of the PTB biotic crisis. – Global and Planetary Change 55: 155–176.

Kozur, H. & Pjatakova, M. 1976. Die Conodontenart *Anchignathodus parvus* n. sp., eine wichtige Leitform der basalen Trias. – Koninklijke Nederlandse Akademic van Wetenschappen, Proceedings, Series B 79 (2): 123–128.

Krull, E. S. & Retallack, G. J. 2000. $\delta^{13}C$ depth profiles from paleosols across the Permian–Triassic boundary: Evidence for methane release. – Geological Society of America Bulletin 112: 1459–1472.

Krull, E. S., Retallack, G. J., Campbell, H. J. & Lyon, G. L. 2000. $\delta^{13}C_{org}$ chemostratigraphy of the Permian–Triassic boundary in the Maitai Group, New Zealand: Evidence for high-latitudinal methane release. – New Zealand Journal of Geology and Geophysics 43: 21–32.

Kump, L. R. 2003. The geochemistry of mass extinction. *In* Mackenzie, F. T. (ed.). Sediments, diagenesis, and sedimentary rocks. Vol. 7. Treatise of Geochemistry. Elsevier-Pergamon, Amsterdam: pp. 351–367.

Kump, L. R., Pavlov, A. & Arthur, M. A. 2005. Massive release of hydrogen sulfide to the surface ocean and atmosphere during intervals of oceanic anoxia. – Geology 33: 397–400.

Leonardi, P. 1967. Le Dolomiti. Geologia dei monti tra Isarco e Piave. 3 volumi. Manfrini, Rovereto.

Magaritz, M., Bär, R., Baud, A. & Holser, W. T. 1988. The carbon-isotope shift at the Permian/Triassic boundary in the Southern Alps is gradual. – Nature 331: 337–339.

Malkowski, K., Gruszczynski, M., Hoffman, A. & Halas, S. 1989. Oceanic stable isotope composition and a scenario for the Permo–Triassic crisis. – Historical Biology 2: 289–309.

Morante, R. 1996. Permian and Early Triassic isotopic records of carbon and strontium in Australia and a scenario of events about the Permian–Triassic boundary. – Historical Biology 11: 289–310.

Mostler, H. 1982. Bozener Quarzporphyr und Werfener Schichten. *In* Exkursionsführer zur 4. Jahrestagung der Österreichischen Geologischen Gesellschaft, Seis am Schlern, Südtirol, 1982. Innsbruck: pp. 43–79.

Musashi, M., Isozaki, Y., Koike, T. & Kreulen, R. 2001. Stable carbon isotope signature in mid-Panthalassa shallow-water carbonates across the Permo–Triassic boundary: Evidence for ^{13}C-depleted superocean. – Earth and Planetary Science Letters 191: 9–20.

Nan Jun-ya & Liu Yu-yan. 2004. Organic and inorganic carbon-isotope shift and paleoenvironment at the P–T boundary section in Meishan, Zhejiang Province. – Geochimica 33 (1): 9–19 [in Chinese with English abstract].

Newton, R. J., Pevitt, E. L., Wignall, P. B. & Bottrell, S. H. 2004. Large shifts in the isotopic composition of seawater sulphate across the Permo–Triassic boundary in northern Italy. – Earth and Planetary Science Letters 218: 331–345.

Nicora, A. & Perri, M. C. 1999. The P/T boundary in the Tesero section, western Dolomites (Trento), 3.3 Bio- and chronostratigraphy. *In* Stratigraphy and facies of the Permian deposits between Eastern Lombardy and the western Dolomites. Field Trip Guidebook of the Continental Permian International Congress, 15–25 September 1999, Brescia, Italy. Pavia University, Pavia: pp. 97–100.

Noé, S. U. 1987. Facies and Paleogeography of the marine Upper Permian and of the Permian–Triassic boundary in the Southern Alps (*Bellerophon* Formation, Tesero Horizon). – Facies 16: 89–142.

Oberhänsli, H., Hsü, K. J., Piasecki, S. & Weissert, H. 1989. Permian–Triassic carbon-isotope anomaly in Greenland and in the Southern Alps. – Historical Biology 2: 37–49.

Payne, J. L. & Kump, L. R. 2007. Evidence for recurrent Early Triassic massive volcanism from quantitative interpretation of carbon isotope fluctuations. – Earth and Planetary Science Letters 256: 264–277.

Perri, M. C. 1991. Conodont biostratigraphy of the Werfen Formation (Lower Triassic) Southern Alps, Italy. – Bollettino della Società Paleontologica Italiana 30: 23–46.

Racki, G. & Wignall, P. B. 2005. Late Permian double-phased mass extinction and volcanism: an oceanographic perspective. *In* Over, D. J., Morrow, J. R. & Wignall, P. B. (eds). Understanding Late Devonian and Permian–Triassic Biotic and Climatic Events: Towards an Integrated Approach. Cambridge University Press, Cambridge: pp. 263–297.

Rampino, M. R. & Caldera, K. 2005. Major perturbation of ocean chemistry and a 'Strangelove Ocean' after the end-Permian mass extinction. – Terra Nova 17: 554–559.

Raup, D. M. 1991. A kill curve for Phanerozoic marine species. – Paleobiology 17: 37–48.

Renne, P. R., Zichao, Z., Richards, M. A., Black, M. T. & Basu, A. R. 1995. Synchrony and causal relations between Permian–Triassic boundary crises and Siberian flood volcanism. – Science 269: 1413–1416.

Retallack, G. J. & Jahren, A. H. 2008. Methane release from igneous intrusion of coal during Late Permian extinction events. – Journal of Geology 116: 1–20.

Riccardi, A., Kump, L. R., Arthur, M. A. & D'Hondt, S. 2007. Carbon isotopic evidence for chemocline upward excursions during the end-Permian event. – Palaeogeography, Palaeoclimatology, Palaeoecology 248: 73–81.

Sarkar, A., Yoshioka, H., Ebihara, M. & Naraoka, H. 2003. Geochemical and organic carbon isotope studies across the continental Permo–Triassic boundary of Raniganj Basin, eastern India. – Palaeogeography, Palaeoclimatology, Palaeoecology 191: 1–14.

Schindewolf, O. H. 1953. Über die Faunenwende vom Paläozoikum zum Mesozoikum. – Zeitschrift der Deutschen Geologischen Gesellschaft 105: 153–182.

Scholger, R., Mauritsch, H. J. & Brandner, R. 2000. Permian–Triassic boundary magnetostratigraphy from the Southern Alps (Italy). – Earth and Planetary Science Letters 176: 495–508.

Schönlaub, H. P. 1991. The Permian–Triassic of the Gartnerkofel-1 core (Carnic Alps, Austria): Conodont biostratigraphy. – Abhandlungen der Geologischen Bundesanstalt in Wien 45: 79–98.

Sephton, M. A., Looy, C. V., Veefkind, R. J., Brinkhuis, H., de Leeuw, J. W. & Visscher, H. 2002. Synchronous record of $\delta^{13}C$ shifts in the oceans and atmosphere at the end of the Permian. *In* Koeberl, C. & MacLeod, K. G. (eds). Catastrophic Events and Mass Extinctions: Impacts and Beyond. – Geological Society of America Special Paper 356: 455–462.

Sephton, M. A., Looy, C. V., Brinkhuis, H., Wignall, P. B., de Leeuw, J. W. & Visscher, H. 2005. Catastrophic soil erosion during the end-Permian biotic crisis. – Geology 33: 941–944.

Sepkoski, J. J. 1989. Periodicity in extinction and the problem of catastrophism in the history of life. – Journal of the Geological Society 146: 7–19.

Stampfli, G. M. & Borel, G. D. 2002. A plate tectonic model for the Paleozoic and Mesozoic constrained by dynamic plate boundaries and restored synthetic oceanic isochrons. – Earth and Planetary Science Letters 196: 17–33.

Svensen, H., Planke, S., Malthe-Sørenssen, A., Jamtveit, B., Myklebust, R., Eidem, T. R. & Rey, S. S. 2004. Release of methane from a volcanic basin as a mechanism for initial Eocene global warming. – Nature 429: 542–545.

Szurlies, M. 2004. Magnetostratigraphy: the key to a global correlation of the classic Germanic Trias – case study Volpriehausen Formation (Middle Buntsandstein), central Germany. – Earth and Planetary Science Letters 227: 395–410.

Thomas, B. M., Willink, R. J., Grice, K., Twitchett, R. J., Purcell, R. R., Archbold, N. W., George, A. D., Tye, S., Alexander, R., Foster, C. B. & Barber, C. J. 2004. Unique marine Permian–Triassic boundary section from Western Australia. – Australian Journal of Earth Sciences 51: 423–430.

Twitchett, R. J. 2007. Climate change across the Permian/Triassic boundary. *In* Williams, M., Haywood, A. M., Gregory, F. J. & Schmidt, D. N. (eds). Deep-Time Perspectives on Climate Change: Marrying the Signal from Computer Models and Biological Proxies. The Micropalaeontological Society, Special Publications. The Geological Society, London: pp. 191–200.

Twitchett, R. J., Looy, C. V., Morante, R., Visscher, H. & Wignall, P. B. 2001. Rapid and synchronous collapse of marine and terrestrial ecosystems during the end-Permian biotic crisis. – Geology 29: 351–354.

Visscher, H., Brinkhuis, H., Dilcher, D. L., Elsik, W. C., Eshet, Y., Looy, C. V., Rampino, M. R. & Traverse, A. 1996. The terminal Paleozoic fungal event: Evidence of terrestrial ecosystem destabilization and collapse. – Proceedings of National Academic Science of the United States of America 93: 2155–2158.

Wang, K., Geldsetzer, H. H. J. & Krouse, H. R. 1994. Permian–Triassic extinction: Organic $\delta^{13}C$ evidence from British Columbia, Canada. – Geology 22: 580–584.

Wignall, P. B. 2007. The End-Permian mass extinction – how bad did it get? – Geobiology 5: 303–309.

Wignall, P. B. & Hallam, A. 1992. Anoxia as a cause of the Permian/Triassic mass extinction: Facies evidence from northern Italy and the western United States. – Palaeogeography, Palaeoclimatology, Palaeoecology 93: 21–46.

Wignall, P. B., Morante, R. & Newton, R. 1998. The Permo–Triassic transition in Spitsbergen: $\delta^{13}C_{org}$ chemostratigraphy, Fe and S geochemistry, facies, fauna and trace fossils. – Geological Magazine 135: 47–62.

Wit, M. J. de, Ghosh, J. G., Villiers, S. de, Rakotosolofo, N., Alexander, J., Tripathi, A. & Looy, C. 2002. Multiple Organic carbon isotope reversals across the Permian–Triassic boundary of terrestrial Gondwana Sequences: Clues to extinction patterns and delayed ecosystem recovery. – Journal of Geology 110: 227–240.

Yin Hong-fu, Zhang Ke-xin, Tong Jin-nan, Yang Zun-yi & Wu Shunbao. 2001. The Global Stratotype Section and Point (GSSP) of the Permian–Triassic Boundary. – Episodes 24 (2): 102–114.

